



## Simple-source model of military jet aircraft noise<sup>1,2</sup>

Jessica Morgan<sup>a)</sup>  
Tracianne B. Neilsen<sup>b)</sup>  
Kent L. Gee<sup>c)</sup>  
Alan T. Wall<sup>d)</sup>  
Brigham Young University  
Department of Physics and Astronomy  
N283 ESC  
Provo, UT 84602

Michael M. James<sup>e)</sup>  
Blue Ridge Research and Consulting LLC  
15 W. Walnut St.  
Asheville, NC 28804

**Described is a method for determining a semi-empirical, equivalent simple-source model that accounts for the aeroacoustic sources in the jet plumes of high-performance military aircraft. The characteristics of the equivalent source are guided by previously reported observations of jet noise, including an asymmetric, partially correlated source distribution and known far-field peak directivity angle. The parameters of the equivalent source model are chosen to reproduce the data recorded on large planar apertures in the near-field of an F-22A Raptor. Peak axial locations and relative contributions of the correlated and uncorrelated portions of the equivalent source are chosen to replicate the directionality and**

---

<sup>1</sup> SBIR DATA RIGHTS - (DFARS 252.227-7018 (JUNE 1995)); Contract Number: [FA8650-08-C-6843](#);  
Contractor Name and Address: [Blue Ridge Research and Consulting, LLC, 15 W Walnut St. Suite C, Asheville, NC](#)  
Expiration of SBIR Data Rights Period: [March 17, 2016](#) (Subject to SBA SBIR Directive of September 24, 2002)  
*The Government's rights to use, modify, reproduce, release, perform, display, or disclose technical data or computer software marked with this legend are restricted during the period shown as provided in paragraph (b)(4) of the Rights in Noncommercial Technical Data and Computer Software—Small Business Innovation Research (SBIR) Program clause contained in the above identified contract. No restrictions apply after the expiration date shown above. Any reproduction of technical data, computer software, or portions thereof marked with this legend must also reproduce the markings.*

<sup>2</sup> Distribution A – Approved for Public Release; Distribution is Unlimited 88ABW-2011-5646

<sup>a)</sup> email: [jessredmorg@gmail.com](mailto:jessredmorg@gmail.com)

<sup>b)</sup> email: [tbn@byu.edu](mailto:tbn@byu.edu)

<sup>c)</sup> email: [kentgee@byu.edu](mailto:kentgee@byu.edu)

<sup>d)</sup> email: [alantwall@gmail.com](mailto:alantwall@gmail.com)

<sup>e)</sup> email: [michael.james@blueridgeresearch.com](mailto:michael.james@blueridgeresearch.com)

**extent of the sound field. The source characteristics, although based on matching data at one measurement plane, are able to approximate the radiation at other near and mid-field locations.**

## 1 INTRODUCTION

This paper describes the development of an equivalent source model (ESM) using simple sources to predict the radiation of jet noise produced by military jet aircraft. Development of such a model has at least two benefits. First, the near-aircraft environment can be predicted, which is beneficial in establishing auditory risk, e.g., for flight crew personnel working on an aircraft carrier deck. Second, an ESM can be evaluated in a computationally efficient manner, which allows the effects of individual parameters to be examined. This can result in a better understanding of source characteristics that are important to the radiation, lending at least indirect insight into the aeroacoustic properties of the hot, turbulent flow.

An ESM is a data-based, source-characterization method<sup>1</sup> that utilizes some *a priori* knowledge of, or assumption regarding, the source characteristics.<sup>2</sup> From this assumption, a distribution of equivalent sources is created. The recorded data are then used to find approximate source strengths for each of the assumed sources from which the radiated field is calculated. However, this distribution is non-unique. (Lighthill's<sup>3,4</sup> famous aeroacoustic analogy, in which the jet noise source is described mathematically as a set of quadrupoles, could be viewed as an ESM.) In an ESM, obtaining the source strengths can be accomplished with a least-squares inversion to match the measured field. For example, Shafer<sup>5</sup> used the measured complex pressure field along a hemisphere to equivalently represent the radiation by an axial cooling fan as a collection of 19 monopoles. On the other hand, development of an ESM can also be done empirically. For example, an oft-used model in launch vehicle noise involves assigning a sound power distribution to a collection of uncorrelated sources and then applying directivity curves to the radiation.<sup>6-8</sup> McLaughlin *et al.*<sup>9</sup> also developed an uncorrelated, symmetric source distribution in examining the impact of a ground reflecting plane on model-scale jet noise. Another aeroacoustically related ESM study is that of Holste,<sup>10</sup> who applied ring-like equivalent sources to the sound radiation from engine ducts.

In developing an ESM for high-power military jet aircraft noise, one must consider the various source characteristics that should guide the development of a model. First, jet noise source are distributed over some volume downstream of the nozzle. Second, a heated, supersonic jet appears to have an asymmetric axial source distribution, with a rapid onset followed by a slower decay downstream.<sup>6,7,11,12</sup> Third, the noise field is partially correlated, owing to the finite correlation lengths of the turbulent structures. This has led to a two-source description of jet noise by Tam and others.<sup>13,14</sup> Specifically, fine-scale turbulence results in a distribution of uncorrelated, omnidirectional sources throughout the plume, while large-scale turbulence structures produce more correlated radiation that has a preferred far-field directivity angle. Because the jet characteristics changes as a function of frequency, the ESM development must be treated on a frequency-by-frequency basis.

One characteristic of high-power military jet aircraft noise that is neglected explicitly in this study is that of nonlinear propagation. Gee *et al.*<sup>15,16</sup> have shown that the far-field, noise propagation from the F-22A is nonlinear at intermediate and high engine powers. However, because nonlinear effects were most readily manifested at frequencies above 1 kHz and large propagation distances, a linearized ESM at low to moderate frequencies, close to the plume, is worthwhile.

In this paper, an ESM for the noise radiated by the F-22A Raptor is described. The model is based on data collected during an extensive field experiment.<sup>17</sup> Following a summary of the measurements, results of creating and applying the simple-source ESM are shown and discussed for the 315 Hz one-third octave band with one engine at afterburner. The findings demonstrate the promise equivalent source methods hold in modeling jet noise fields and leading to a better understanding of source characteristics.

## 2 FULL-SCALE EXPERIMENT

In July 2009, researchers at Brigham Young University and Blue Ridge Research and Consulting took extensive noise measurements of an F-22A Raptor at Holloman Air Force Base. The jet was tied down to a concrete run-up pad and cycled through four engine power conditions: idle, intermediate, military, and afterburner. A complete description of the experiment is found in Ref. [17].

The data analyzed in this study were recorded on the rectangular array of microphones shown in Fig. 1. The 90 microphones were 15.2 cm (6.0 in) apart and covered an aperture 0.6 m high by 2.6 m (2 ft x 8.5 ft) long. The rig that held the microphones was positioned at ten locations along a 22.9 m (75 ft)-long track. The rig was also adjusted to three heights during the experiment, with the center of the array at 0.7, 1.3 and 1.9 m (27, 51, and 75 in). When the rig was moved to a different position for a new scan, it was positioned such that several microphones overlapped the previous scans. When the data from the 30 scans are pieced together, they yield a 1.8 m x 22.9 m (6 ft by 75 ft) measurement plane.

The track was moved to the different locations as illustrated in Fig. 2 by the solid black lines. The red triangles along the track indicate the locations of the center of the microphone array for subsequent measurement scans. The set of measurements obtained 4.1 m from the shear layer of the jet plume are referred to as plane 1 data, while plane 2 data comes from measurements taken 5.6 m from the shear layer of the jet plume. Data along both measurement planes 1 and 2 are taken at the three heights and ten horizontal positions described in the previous paragraph. Additionally, measurements were taken along an arc, in ten degree increments, where the rig was 22.9 m (75 ft) away from the estimated peak source location,<sup>24</sup> marked with a green “x” in Fig. 2. The height of the center of the array was 1.9 m (75 in) for the arc measurements.

## 3 MATHEMATICAL DEVELOPMENT

The main purpose of this study is to show the plausibility of using a semi-empirical, simple-source model to provide an equivalent source for jet aircraft noise. This section introduces the mathematical development behind creating this model’s equivalent source. The next section shows how each component of the model contributes to the whole and compares to the measured data.

The model’s equivalent source is based on a distribution of monopoles. The arrangement and relative amplitudes of the monopoles determines the overall radiation pattern. Individually, each monopole radiates pressure omnidirectionally, and the complex pressure amplitude from a time-harmonic monopole source is

$$\tilde{P} = \frac{\tilde{A}e^{-jkR}}{R} = \tilde{A}G(\vec{r}, \vec{r}_0), \quad (1)$$

where  $\tilde{A}$  is a complex amplitude,  $R = |\vec{r} - \vec{r}_0|$ ,  $k$  is the wave number for a given frequency and  $j$  is the complex number  $\sqrt{-1}$ . In this model,  $\vec{r}_0$  is the variable source location, and  $\vec{r}$  corresponds to the microphone locations in the measured data. The pressure is also expressed in Eqn. (1) using the Green's function,  $G(\vec{r}, \vec{r}_0)$ , where dependence on frequency or wavenumber,  $k$ , is implicit. In this model,  $\vec{r}_0$  is the variable source location, and  $\vec{r}$  corresponds to the microphone locations in the measured data.

A key factor in modeling the noise of a source in a realistic environment is to include effects of reflections, e.g. from the ground. For this ESM, the interference pattern produced by the direct noise and ground-reflected noise provides useful information about the position and distribution of the equivalent sources. Figure 3 illustrates how the direct source and its image source radiate to the measurement plane. The radiation pattern shown in Fig. 3 is the SPL measured for the 315-Hz, one-third octave band, along measurement plane 2 in Fig. 2. The noise along the measurement plane shows evidence of a strong interference null. The orientation of this null can be used to guide the development of an equivalent source based on the coherent interaction of direct and image sources. The current ESM approach is developed using line arrays of monopoles along the centerline of the jet and their images. This differs from the approach in Ref. [9] where they calculated a free-field, beamformed source distribution for a laboratory-scale jet and applied it to the case with a ground-reflecting plane.

The addition of an image source to the monopole's complex pressure amplitude in Eqn. (1) gives

$$\tilde{P} = \tilde{A}[G(\vec{r}, \vec{r}_D) + \tilde{Q}G(\vec{r}, \vec{r}_I)], \quad (2)$$

where  $\vec{r}_D$  is the direct source vector and  $\vec{r}_I$  is the image source vector. The spherical wave reflection coefficient,  $\tilde{Q}$ , determines the amplitude and phase of the image source relative to the direct source. Although  $\tilde{Q}$  is generally a complex quantity that depends on a number of factors, including frequency, ground impedance, and angle of incidence,<sup>18</sup>  $\tilde{Q} = 1$  is used in this particular study, which corresponds to an infinite impedance, i.e., rigid ground.

Equation (2) gives the complex pressure from a single monopole with a ground reflection and, with appropriate values of  $\tilde{A}$ ,  $\vec{r}_D$ , and  $\vec{r}_I$ , is a "first-order" approximation to the location of the dominant equivalent source for the jet plume. A more accurate representation of the jet noise sources is obtained by including a line array of monopole sources with a smoothly varying amplitude distribution. The total complex pressure from an array of discrete monopoles over a reflecting plane is

$$P = \sum_{m=1}^N A_m [G(\vec{r}, \vec{r}_{D_m}) + \tilde{Q}_m G(\vec{r}, \vec{r}_{I_m})] , \quad (3)$$

where  $\tilde{A}_m$  is the relative amplitude of the  $m^{\text{th}}$  monopole, and  $N$  is the total number of monopoles in the array. Although the spherical reflection coefficient  $\tilde{Q}_m$  may be different for each monopole, they are all set equal to one for the model considered here.

The amplitude distribution for the model,  $\tilde{A}_m$ , is chosen to represent observed properties of jet noise. Prior research on model-scale jets indicates that the strength of the sources within the jet plume do not follow a symmetric distribution (e.g., see Figs. 1, 5-6 in Ref. [11]). Phased-array analyses on a full-scale, high-power jet engine also suggest an asymmetric source distribution along the axis of the jet plume (cf. Fig. 11(a) in Ref. [12]). In addition, computational fluid dynamics calculations by Haynes *et al.*<sup>8</sup> for the turbulent velocity

fluctuations within a large solid rocket motor plume supports an asymmetric source distribution developed by Vanier.<sup>7</sup> In all three cases—the model-scale jets, the full-scale jet engine, and the large solid rocket motor plume—an asymmetric distribution with a rapid rise and slow decay better imitates the source characteristics in the jet plume. While several well-known distributions have these characteristics, a Rayleigh distribution was chosen for this particular ESM.

A Rayleigh distribution gives the relative amplitudes of the monopoles as

$$|\tilde{A}_m(z_m, \Delta z, \sigma)| = A_{\max} \frac{z_m - \Delta z}{\sigma^2} e^{-\frac{(z_m - \Delta z)^2}{2\sigma^2}} = A_m(z_m, \Delta z, \sigma), \quad (4)$$

where  $z_m$  is the location of the  $m^{\text{th}}$  monopole,  $A_{\max}$  is the peak amplitude in the distribution,  $\Delta z$  is distance the peak of the distribution has been shifted downstream, and  $\sigma$  is the relative width of the distribution. As shown in Fig. 4, the shift distance,  $\Delta z$ , corresponds with the placement of the peak in the Rayleigh distribution downstream to desired location,  $z$ . In modeling the jet noise source, the relative amplitudes of the line array of monopoles at the measurement plane are controlled by the source parameters in Eqn. (4).

In addition to the asymmetry of the source distribution, another characteristic of jet noise that the model must account for is the presence of both correlated and uncorrelated noise. This is accomplished by combining two line arrays of monopoles: one correlated and one uncorrelated. For the uncorrelated source, the total squared pressure is calculated by adding up the contribution of the monopoles incoherently:

$$P_{T,u}^2 = \sum_{m=1}^N [A_{m,u} [G(\vec{r}, \vec{r}_{D_m}) + \tilde{Q}_m G(\vec{r}, \vec{r}_{I_m})]]^2, \quad (5)$$

where the subscript  $u$  denotes that this is uncorrelated contribution to the field. In the uncorrelated line array, each monopole radiates at random with respect to the rest of the monopoles.

On the other hand, the correlated line array is assigned a fixed phase relationship among the monopole amplitudes. By properly assigning the phases, it is possible to steer the sound in a desired direction. The correlated line array of monopoles is responsible for modeling the jet plume's observed far-field directivity of the sound radiation (at an angle  $\theta$  relative to the nozzle and jet centerline).<sup>11</sup> To include this physical observation in the model, the phases are defined in the amplitude distribution as

$$\tilde{A}_m(z_m, \Delta z, \sigma) = A_m(z_m, \Delta z, \sigma) e^{j\varphi m}, \quad (6)$$

where  $\varphi$ , the phase difference, from one monopole to the next is

$$\varphi = \frac{2\pi f d \sin \theta}{c}, \quad (7)$$

and the space between the monopoles,  $d$ , is small enough to simulate a continuous source. (The sound speed is represented in Eqn. (7) by the variable  $c$ .) The far-field directivity angle  $\theta$  can be obtained from analyzing a jet's far-field directivity pattern or can be included as independent parameter. The directivity angle is a function of the engine power and frequency. In the case of correlated sources, the total squared pressure is the coherent sum over the individual monopoles:

$$P_{T,c}^2 = [\sum_{m=1}^N \tilde{A}_{m,c} [G(\vec{r}, \vec{r}_{D_m}) + \tilde{Q}_m G(\vec{r}, \vec{r}_{I_m})]]^2, \quad (8)$$

where the subscript  $c$  denotes a correlated source.

The correlated and uncorrelated line arrays are combined to give the total squared pressure:

$$P_T^2 = P_{T,c}^2 + P_{T,u}^2. \quad (9)$$

This total, modeled, squared pressure is propagated via the Green's function to multiple observation points, which correspond to the microphone locations, and yields a planar map of the sound field to compare with the measured data. The model's parameters are adjusted to create a source that gives the least error between the model and measured data.

The error between the modeled sound field and the measured values is computed by averaging the absolute difference, on a point-by-point basis, between the model and measured data. The error is defined as

$$\text{Error} = 10 \log_{10} \left( \frac{\sum_{i=1}^{\tilde{N}} |\tilde{P}_{r,i}^2 - \tilde{P}_{m,i}^2|}{\sum_{i=1}^{\tilde{N}} \tilde{P}_{r,i}^2} \right), \quad (10)$$

where  $\tilde{P}_{r,i}$  is the reference pressure from the measured data and  $\tilde{P}_{m,i}$  is the model's calculated pressure at measurement location  $i$ .<sup>19</sup> Because the model tends to overestimate the depth of the interference nulls, the summation over  $\tilde{N}$  includes only points with measured levels within a 10 dB range of the maximum SPL at that plane. Not only does this reduce the contribution of the nulls to the total error, but it also emphasizes model agreement with the largest SPL values, which is our primary concern. Since the error is evaluated on a log scale as a decibel, the set of modeling parameters that yields the largest negative value of the error is the best fit.

To find a good fit between the model and the data, multiple parameters are adjusted, on a trial and error basis, to achieve the lowest possible error value. Specifically, peak source location, type of distribution, width of the distribution, relative amplitudes of the correlated and uncorrelated sources, and directivity angle are selected. For this work, the distribution is assumed to be a Rayleigh distribution, and the directivity angle,  $\theta$ , is chosen based on previous far-field directivity measurements.<sup>15,20</sup> The modeled line arrays are positioned on the jet plume centerline and at the height of the nozzle, about two meters above ground. This leaves four adjustable parameters for creating an ESM that is intended to represent the jet's radiated noise at a particular frequency: the distribution's width,  $s$ , the peak location,  $z_p$ , and the relative amplitudes,  $A_{m,c}$  and  $A_{m,u}$ , of the correlated and uncorrelated sources. Note that this approach utilizes the ground-reflected data to directly produce a partially-correlated, asymmetric source distribution, where the work reported in Ref. [9] utilized free-field source estimates to obtain an uncorrelated, symmetric source distribution.

#### 4 INITIAL APPLICATION OF MODEL

The implications of each step in the modeling process are now presented. As an example, the model is used to replicate the 315-Hz, one-third-octave band data measured on plane 2 while the F-22A was operating at afterburner. The parameters that characterize the equivalent source are the standard deviation and location of the peak in the distribution and the relative amplitudes

of the correlated to uncorrelated sources. These are adjusted to produce a modeled source distribution with the least error according to Eqn. (10).

Figure 5 shows the SPL computed for the one-third-octave band centered at 315 Hz for each of the components of the model separately and how they combine to produce the overall modeled field. Figure 5(a) shows the SPL generated by a monopole at  $z_p = 2.2$  m, which best matches the alignment of the interference null in the data. The remaining parts of Fig. 5 contain the one-third-octave band SPL maps produced by (b) the uncorrelated source alone, (c) the correlated source alone, (d) the total modeled field from the sum of (b) and (c), and (e) the measured data at afterburner. Figure 5(f) gives the absolute difference in decibel between the total modeled field and measured data at each measurement position.

The SPL map shown in Fig. 5(b) comes from Eqn. (5) for an uncorrelated line array source. The “+” on the SPL map marks the downstream location of the peak in the Rayleigh distribution,  $z_p = 2.2$  m. The uncorrelated line array’s source distribution amplitude,  $A_{m,u}$ , is relatively small, but the uncorrelated line array source broadens the null, compared to the monopole case, and contributes to the sideline radiation of the jet.

Equation (8) for a correlated line array source creates the SPL in Fig. 5(c), where the circle on the SPL map marks the projected downstream location of the peak in the Rayleigh distribution,  $z_p = 2.2$  m. The phases  $\phi$ , calculated from Eqn. (7), control the steering of the correlated source. For this frequency,  $125^\circ$  is used for the directivity angle, based on previously measured far-field directivity data.<sup>15,20</sup> The correlated source produces highly directional noise and contributes significantly to the downstream radiation.

The total modeled one-third-octave band SPL in Fig. 5(d) comes from adding together the squared pressures from the correlated and uncorrelated sources, as in Eqn. (9), and then converting to level. A comparison of the modeled results in Fig. 5(b)-(d) to the data in Fig. 5(e) reinforces the point that both the correlated and uncorrelated portions of the model are required to match the spatial distribution of noise recorded near the F-22A. The absolute value of the difference between the model's SPL (Fig. 5(d)) and the measured data's SPL (Fig. 5(e)) is defined as the decibel error and is shown in Fig. 5(f). Outside the region of the interference null there is uniformly less than 3 dB error. The areas of least agreement align with the null because the model grossly over predicts the depth of the interference null. This over prediction could be lessened by adding a random volumetric component (without a corresponding coherent ground reflection) to the model to represent the 3-dimensional extent of the jet plume. Table 1 lists the overall error values from each part of the model when compared to the measured data: a combination of correlated and uncorrelated sources is necessary to get the least error between the modeled results and the measured data. Other than the over prediction of the null’s depth, there is good agreement between the model and measured data.

Overall the model yields an ESM for jet noise that can predict levels and SPL distributions in a large spatial region with the need to specify only a few parameters for each frequency. This section has described applying the model to one set of the measured data to create an equivalent source. However, for the resulting equivalent source to be considered representative of the noise sources within the jet plume, it needs to be able to predict the radiated field at other locations. By applying the parameters chosen to match the data along plane 2, referred to as the construction plane, to predict the field both closer to (plane 1) and farther from (the arc) the source, the capability of the model to yield equivalent source characteristics that can be used to predict the fields at locations other than the original construction plane is demonstrated. Figure 10 shows the three measurement locations: plane 1, plane 2 and the arc. Figure 10(a) contains the model's predictions and (b) displays the measured data. Table 2 shows the total error values at each of the measurement planes. Although the construction plane has the least error, the fields

predicted at other locations still prove to be reasonable. The SPL along the arc in Fig. 10(a) shows that the amplitude of the modeled noise rolls off correctly in both the upstream and downstream directions. This confirms that the angle of 125 degrees used from the known far-field directivity pattern<sup>15</sup> for the afterburner engine condition was a good choice. This example indicates the flexibility of the model in predicting the spatial variation of the noise levels at different locations in the near and mid fields.

## 6 CONCLUSIONS

In summary, this equivalent source model (ESM) is able to approximate jet-noise phenomena measured along a planar aperture. The combination of a correlated and an uncorrelated line arrays of simple sources with Raleigh-distributed amplitudes reproduce the sound radiated from an F-22A Raptor to within 3 dB, except near the interference nulls. More importantly, the ESM parameters chosen to match the data on one measurement plane also give reasonable results for the radiated field at additional distances from the jet. Additional comparisons as a function of frequency and engine condition will be reported in the future.<sup>21</sup>

## 7 ACKNOWLEDGEMENTS

The authors gratefully acknowledge funding from the Air Force Research Laboratory through the SBIR program and support through a Cooperative Research and Development Agreement (CRADA) between Blue Ridge Research and Consulting LLC, Brigham Young University, and the Air Force.

## 8 REFERENCES

1. M. Ochmann, "The source simulation technique for acoustic radiation problems," *Acustica* **81**, 512–527 (1995).
2. N. P. Valdivia and E. G. Williams, "Study of the comparison of the methods of equivalent sources and boundary element methods for near-field acoustic holography," *J. Acoust. Soc. Am.* **120**, 3694–3705 (2006).
3. M. J. Lighthill, "On Sound generated aerodynamically. Part 1. General Theory," *Proc. R. Soc. London*, **211**, 564-587 (1952).
4. F. Farassat, M. J. Doty, and C. A. Hunter, "The acoustic analogy – A powerful tool in aeroacoustics with emphasis on jet noise prediction, AIAA paper AIAA-2004-2872, May 2004.
5. B. M. Shafer, "Error sensor placement for active control of an axial cooling fan," MS thesis, Brigham Young University, 2007.
6. K. M. Eldred, "Acoustic Loads Generated by the Propulsion System", NASA SP-8072, June 1971.
7. J. Varnier, "Experimental study and simulation of rocket engine freejet noise," *AIAA Journal*, **39**, 1851-1859, October 2001.
8. J. Haynes, and R. Kenny, "Modifications to the NASA SP-8072 Distributed Source Method II for Ares I Lift-Off Environment Predictions," AIAA-2009-3160, 15th AIAA/CEAS Aeroacoustics Conference (30th AIAA Aeroacoustics Conference), Miami, Florida, May 11-13, 2009.
9. D. K. McLaughlin, C.W. Kuo, and D. Papamoschou, "Experiments on the Effect of Ground Reflections on Supersonic Jet Noise," AIAA paper AIAA-2008-22.

10. F. Holste, "An Equivalent Source Method for Calculation of the Sound Radiated from Aircraft Engines", *J. Sound Vibr.*, **203**, 667-695, (1997).
11. C. K. W. Tam, N. N. Pasouchenko, and R. H. Schlinker, "Noise source distribution in supersonic jets," *J. Sound Vib.* **291**, 192-201 (2006).
12. R.H. Schlinker, S.A. Lijenberg, D.R. Polak, K.A. Post, C.T. Chipman, and A.M. Stern, "Supersonic Jet Noise Source Characteristics & Propagation: Engine and Model Scale", *13<sup>th</sup> AIAA/CEAS Aeroacoustics Conf.*, (2007).
13. C. K.W. Tam, K. Viswanathan, K. K. Ahuja, and J. Panda, "The sources of jet noise: Experimental evidence", *J. Fluid Mech.*, **615**, 253-292, (2008).
14. C. K. W. Tam, M. Golebiowski, J. M. Seiner, "On the Two Components of Turbulent Mixing Noise from Supersonic Jets," AIAA paper AIAA-96-1716.
15. K. L. Gee, V. W. Sparrow, M. M. James, J. M. Downing, C. M. Hobbs, T. B. Gabrielson, and A. A. Atchley, "The role of nonlinear effects in the propagation of noise from high-power jet aircraft," *J. Acoust. Soc. Am.* **123**, 4082-4093 (2008).
16. K. L. Gee, V. W. Sparrow, M. M. James, J. M. Downing, C. M. Hobbs, T. B. Babrielson, A. A. Atchley, " Measurement and prediction of noise propagation from a high-power jet aircraft," *AIAA Journal*, **45**, 3003-3006 (2007).
17. A. T. Wall, K. L. Gee, M. M. James, K. A. Bradley, S. A. McNerny, T. B. Neilsen, "Near-field noise measurements of a high-performance military jet aircraft," submitted to *Noise Control Eng. J.* (2011).
18. E. M. Salomons, *Computational Atmospheric Acoustics* (Kluwer Academic Publishers, Norwell, MA, 2001), pp. 123-137.
19. J. Hald, "Basic Theory and properties of statistically optimized near-field acoustical holography," *J. Acoust.Soc. Am.*, **125**, 2105-2120, (2009).
20. Air Force Research Laboratory, NOISEFILE Database, Wright-Patterson AFB, OH, 2003.
21. J. Morgan, T. B. Neilsen, K. L. Gee, A. T. Wall, and M. M. James, "Simple-source model of military jet aircraft noise," submitted to *Noise Control Eng. J.* (2011).

*Table 1 – Error in decibels [as defined in Eqn. (10)] between each part of Fig. 5 (a)-(d) and the measured data (e).*

Fig. 5 Source Type	(a) Single Monopole	(b) Uncorrelated Line Array	(c) Correlated Line Array	(d) Total Model
Error (dB)	-2.7	-0.09	-6.0	-6.2

*Table 2 – Error in decibels [see Eq. (10)] at all three measurement planes for afterburner and 315 Hz.*

Measurement Surface	Plane 1	Plane 2	Arc
Error at 315 Hz	-3.7	-6.1	-4.2



Fig. 1 -The F22A Raptor tied down to the run-up pad with the 90-microphone array shown.

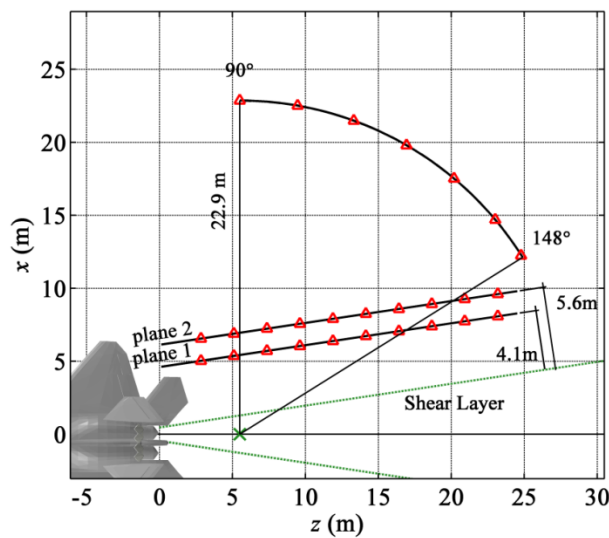


Fig. 2 –Diagram of a portion of the experimental set-up for the acoustical measurements on an F-22A Raptor. The triangles, each 2.3 m apart, mark the center of the microphone array for individual scans. The origin is set at ground level centered below the jet nozzle:  $x$  is the distance away from the jet plume’s centerline,  $y$  is the height off the ground and  $z$  is the distance downstream from the nozzle. The green “x” refers to the estimated peak source location and the reference from which the angles are measured.

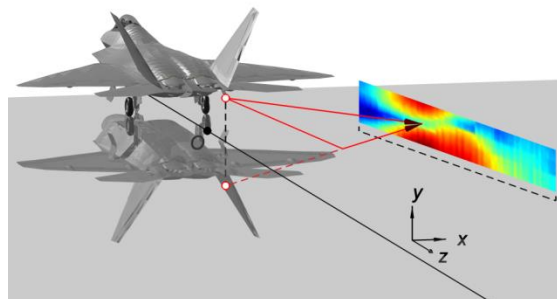


Fig. 3 – A diagram showing the jet plume’s direct source and image source propagating to the measurement plane.

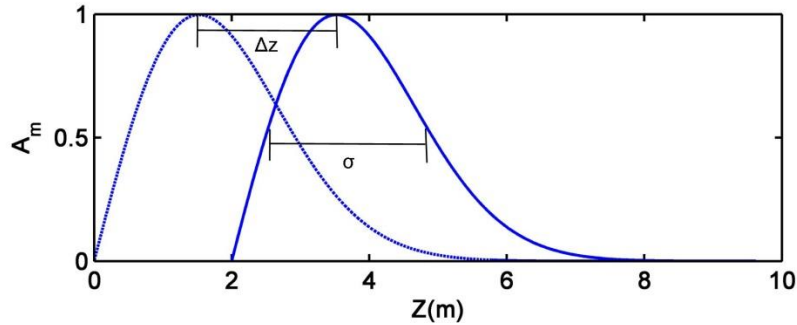


Fig. 4- A Rayleigh distribution (dotted line), which rises quickly and decays slowly, and a shifted distribution (solid line), labeled with the shift distance,  $\Delta z$ , and the standard deviation,  $\sigma$ .

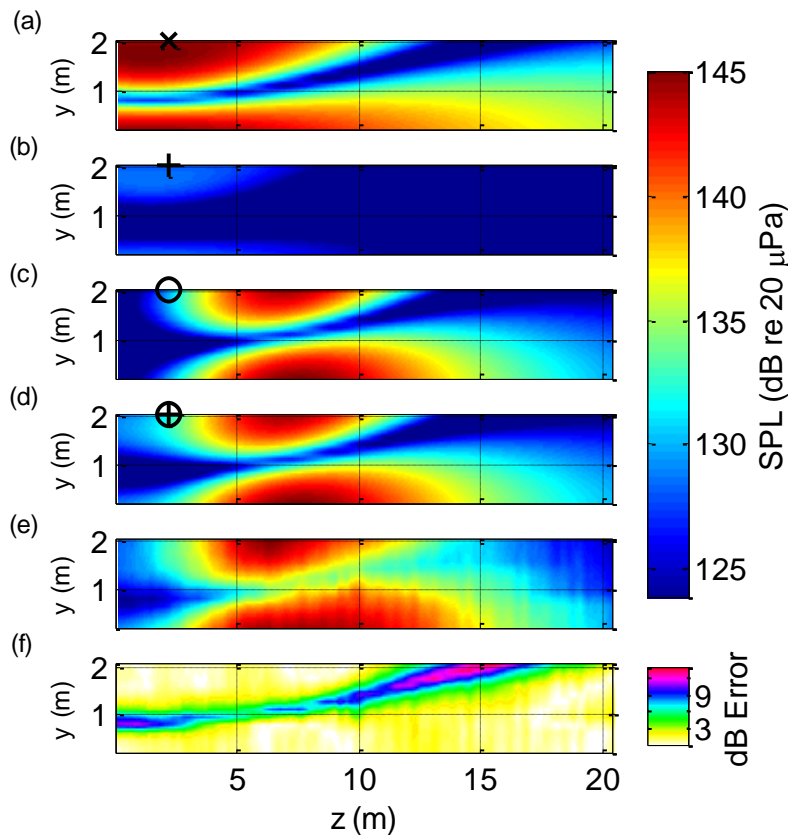


Fig. 5 – SPL for the 315-Hz one-third-octave band modeled on measurement plane 2 (located 5.6 m from the shear layer of the jet plume) with a peak source location  $z_p = 2.2$  m, showing the contribution of different components to the model: (a) a single monopole with its ground reflection, (b) a line array of uncorrelated monopoles, and (c) a line array of correlated monopoles with  $\theta = 125^\circ$ . Part (d) shows the field from the total model, and part (e) contains the F-22A data recorded at afterburner. Part (f) shows the decibel error between (d) and (e).

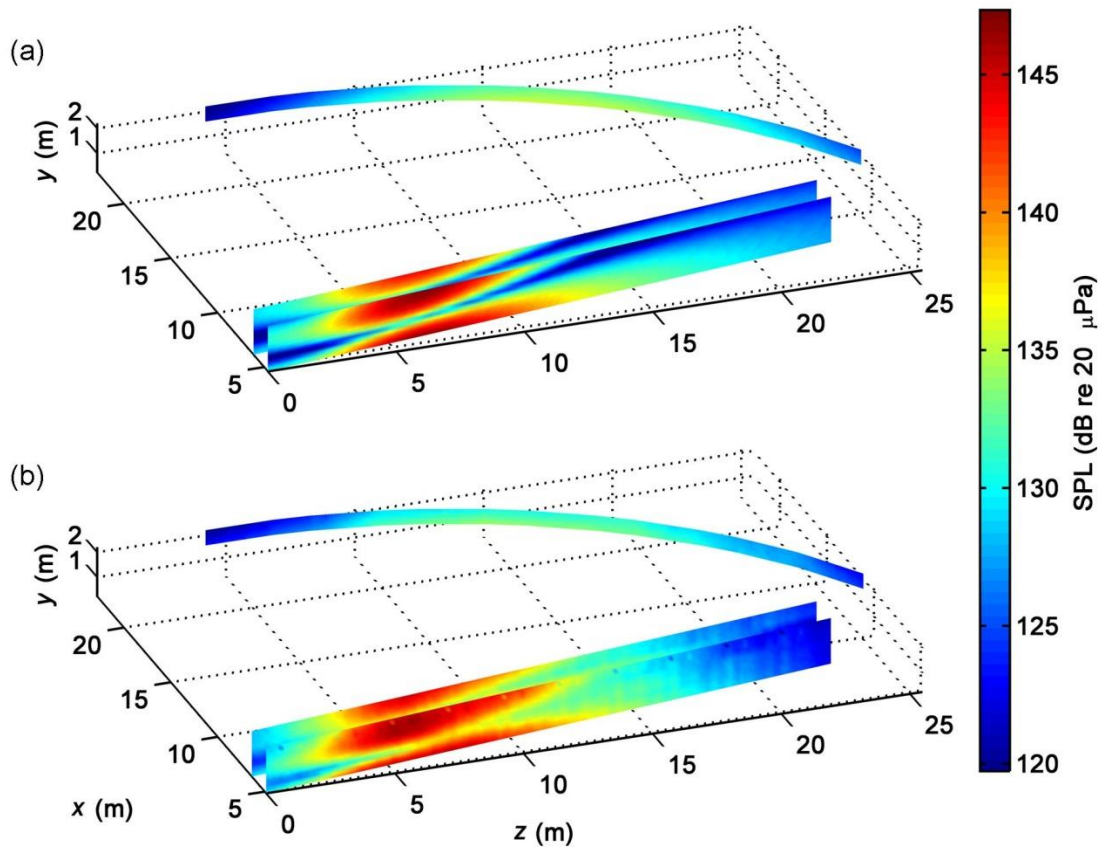


Fig. 6 - 3-D plot showing the 315-Hz one-third-octave band SPL at multiple measurement planes and agreement between model and data at various distances: (a) model using source parameters chosen using plane 2 and (b) measured data at afterburner.